SUPPORTING INFORMATION

Accounting for substrate interactions in the measurement of the dimensions of cellulose nanofibrils

Bruno D. Mattos[†‡], Blaise L. Tardy[†‡*], Orlando J. Rojas[†§*]

[†]Department of Bioproducts and Biosystems, School of Chemical Engineering, Aalto University, P.O. Box 16300, FI-00076 Espoo, Finland

[§]Department of Applied Physics, School of Science, Aalto University, P.O. Box 15100, FI-00076 Espoo, Finland

[‡]These authors contributed equally

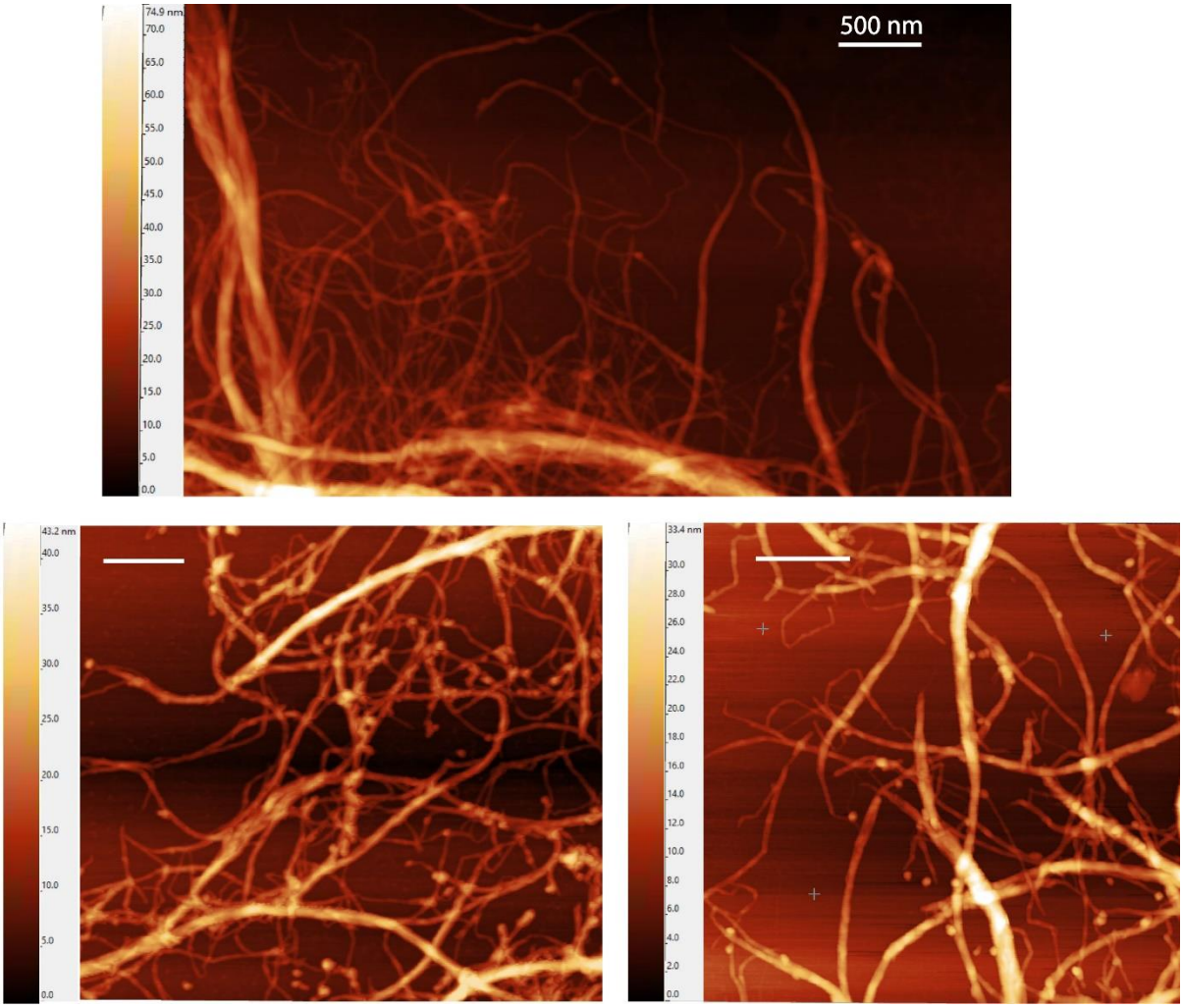

Figure S1. Examples of atomic force microscopy (AFM) images acquired from CNF cast onto PEI-treated mica supports.

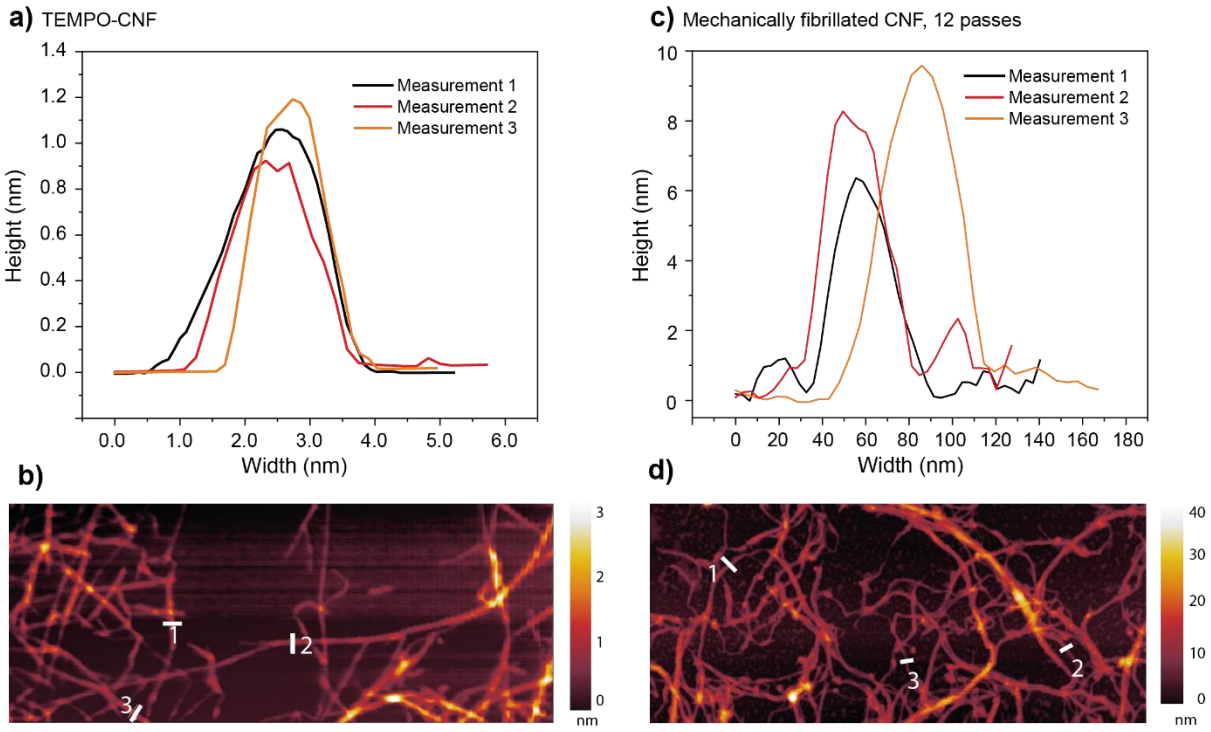

Figure S2. AFM images and height profiles of TEMPO oxidized CNF (a,b) and mechanically fibrillated CNF after 12 passes (c,d).

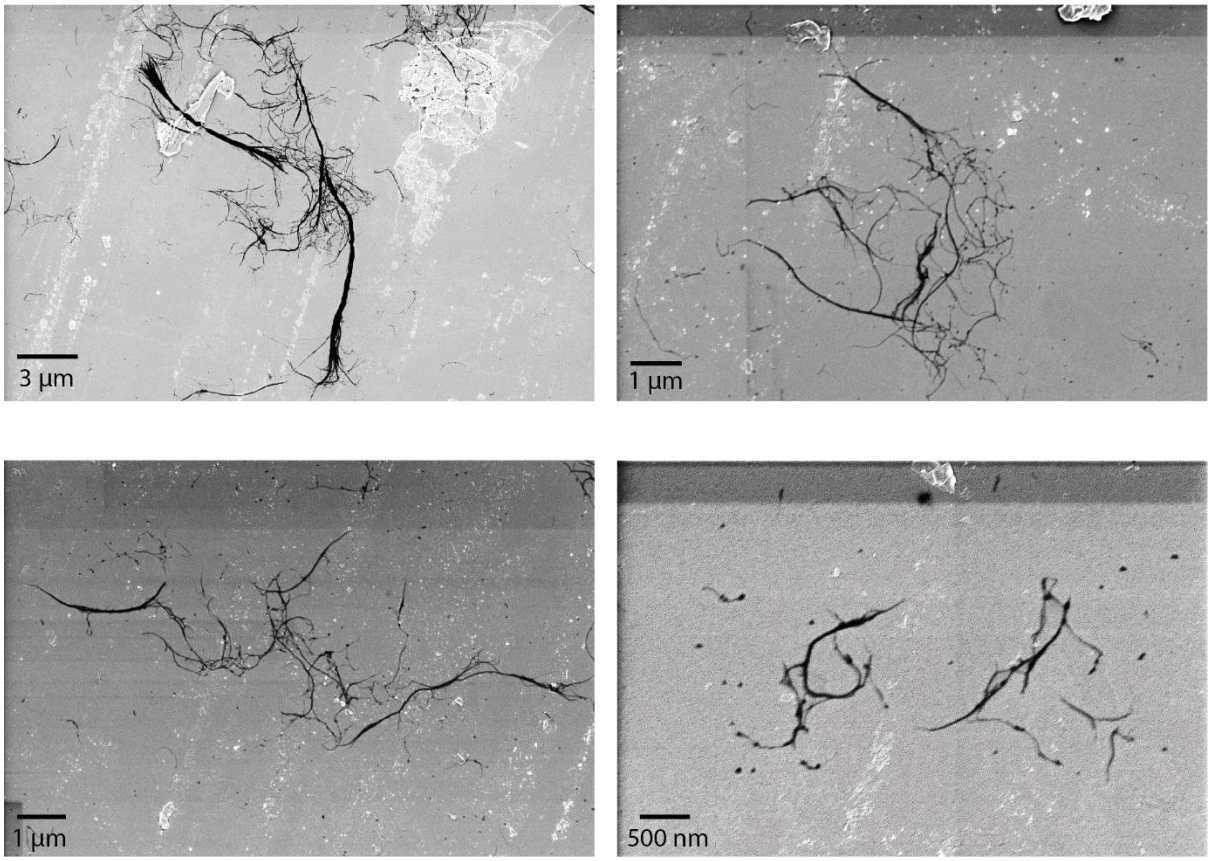

Figure S3. Examples of negative contrast SEM images taken from CNF cast onto PEI-treated iridium surfaces.

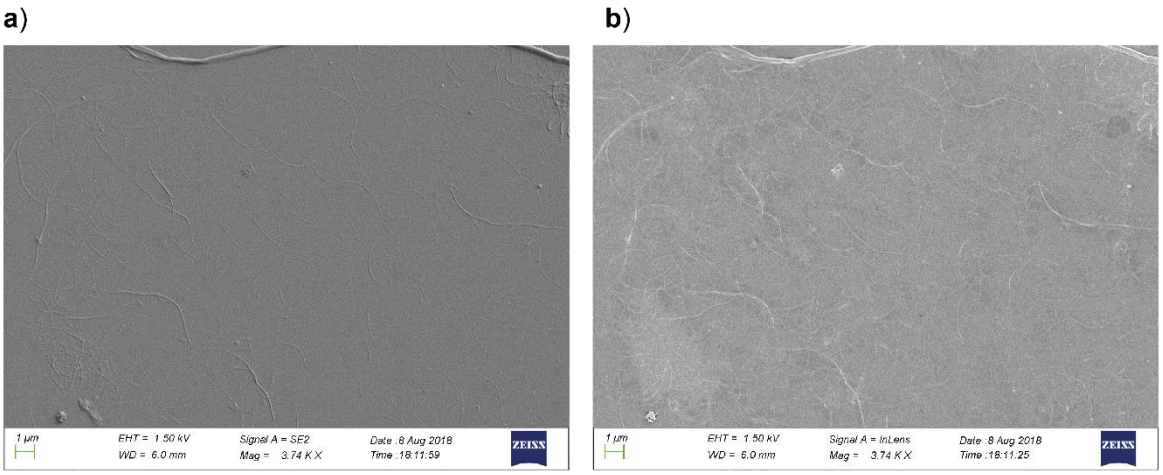

Figure S4. Conventional scanning electron images acquired using the (a) secondary electron and (b) in-lens detectors. PEI-treated mica discs were dip coated with CNF, and then coated with a 4 nm gold layer.

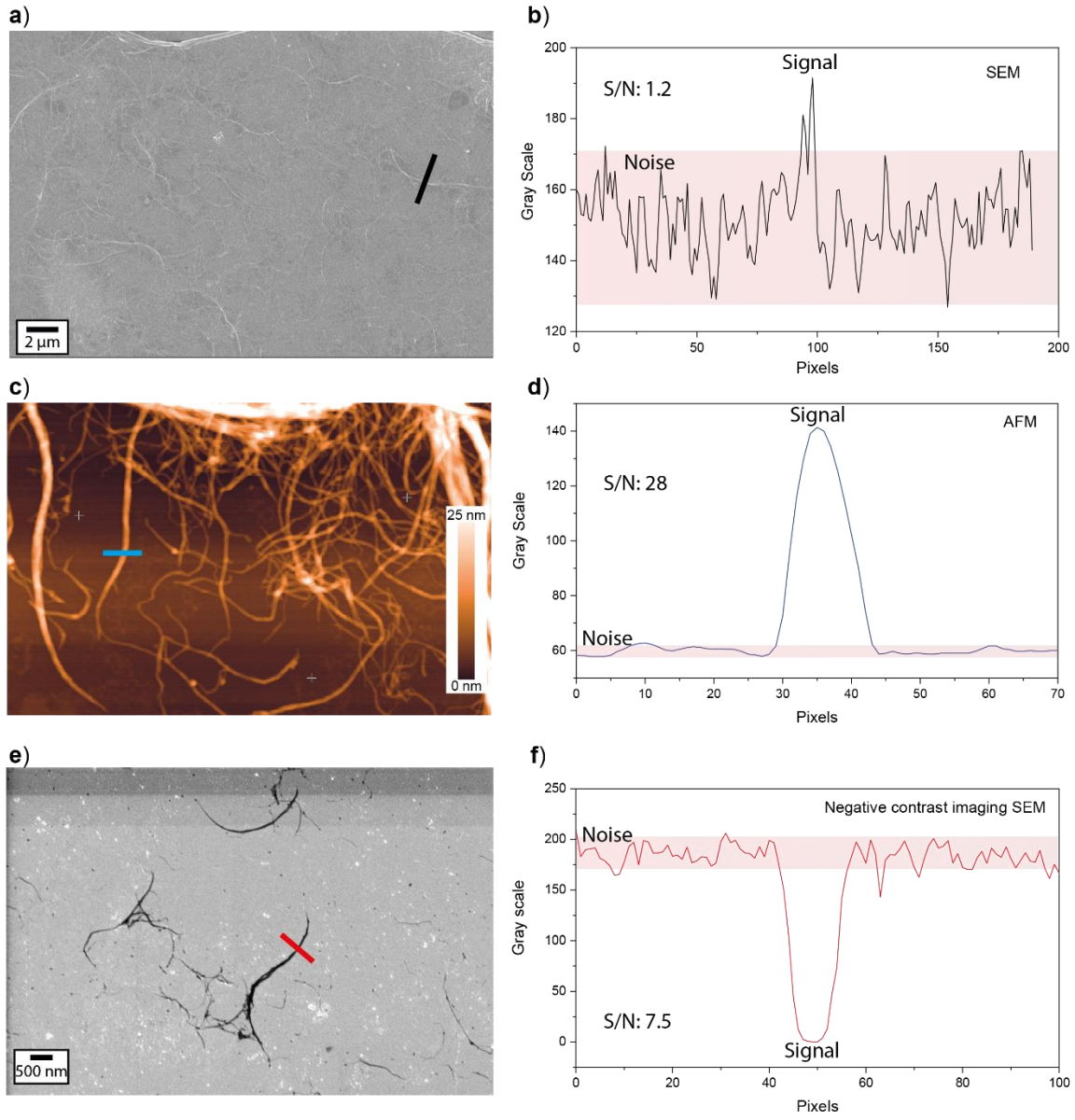

Figure S5. Signal to noise (S/N) ratio determined for the images obtained through the different imaging techniques used. SEM using conventional metal coating of the sample (a), AFM (c), and negative contrast SEM images (e) were used to obtain gray scale profiles (b, d and f, respectively) as an estimate of the signal-to-noise ratio. The gray scale profiles were taken in the lines marked in (a), (c) and (e).

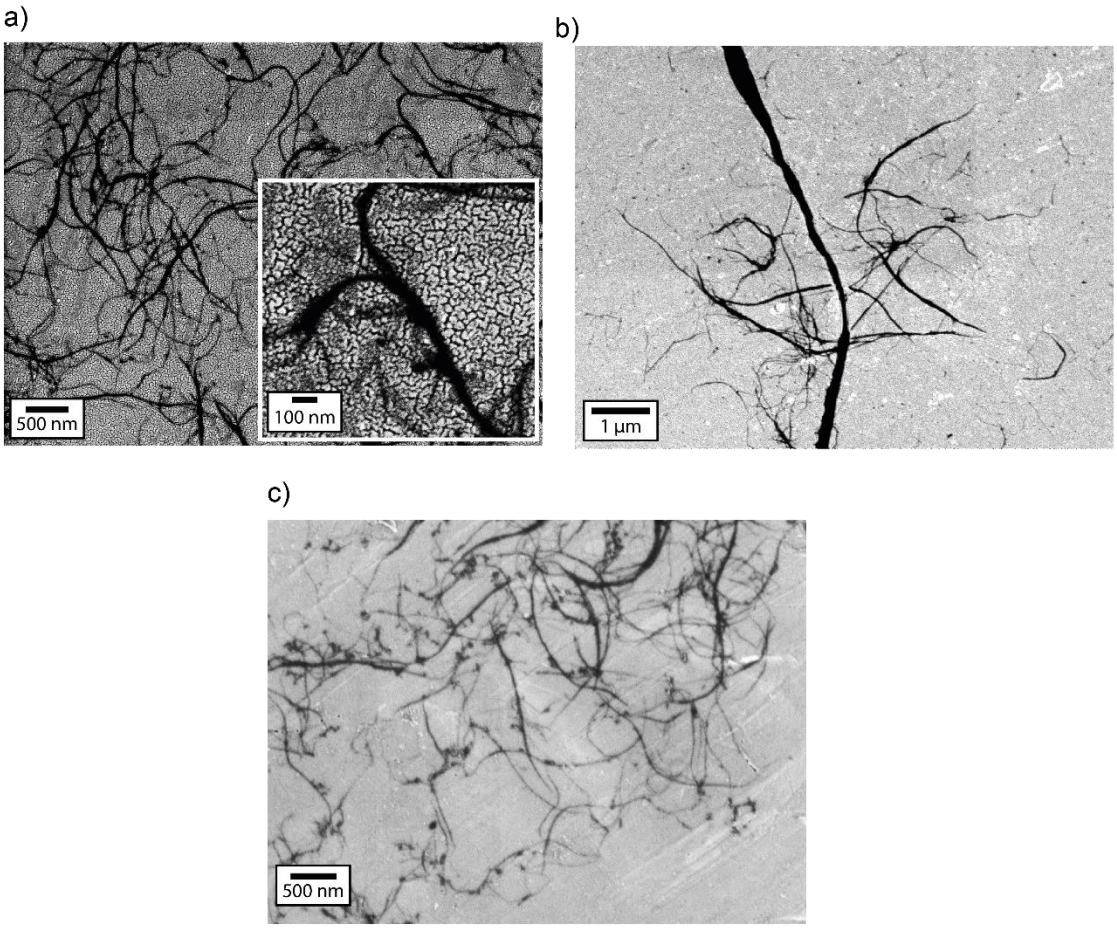

Figure S6. Negative contrast SEM images obtained after dip casting CNF suspension on PEI-treated mica discs previously coated with gold (a) and platinum/palladium alloy (b). The inlet in (a) highlight the grain size of the fractured coating. Panel (c) demonstrates the use of kitchen grade aluminums foil as a conductive substrate for negative contrast imaging in SEM.

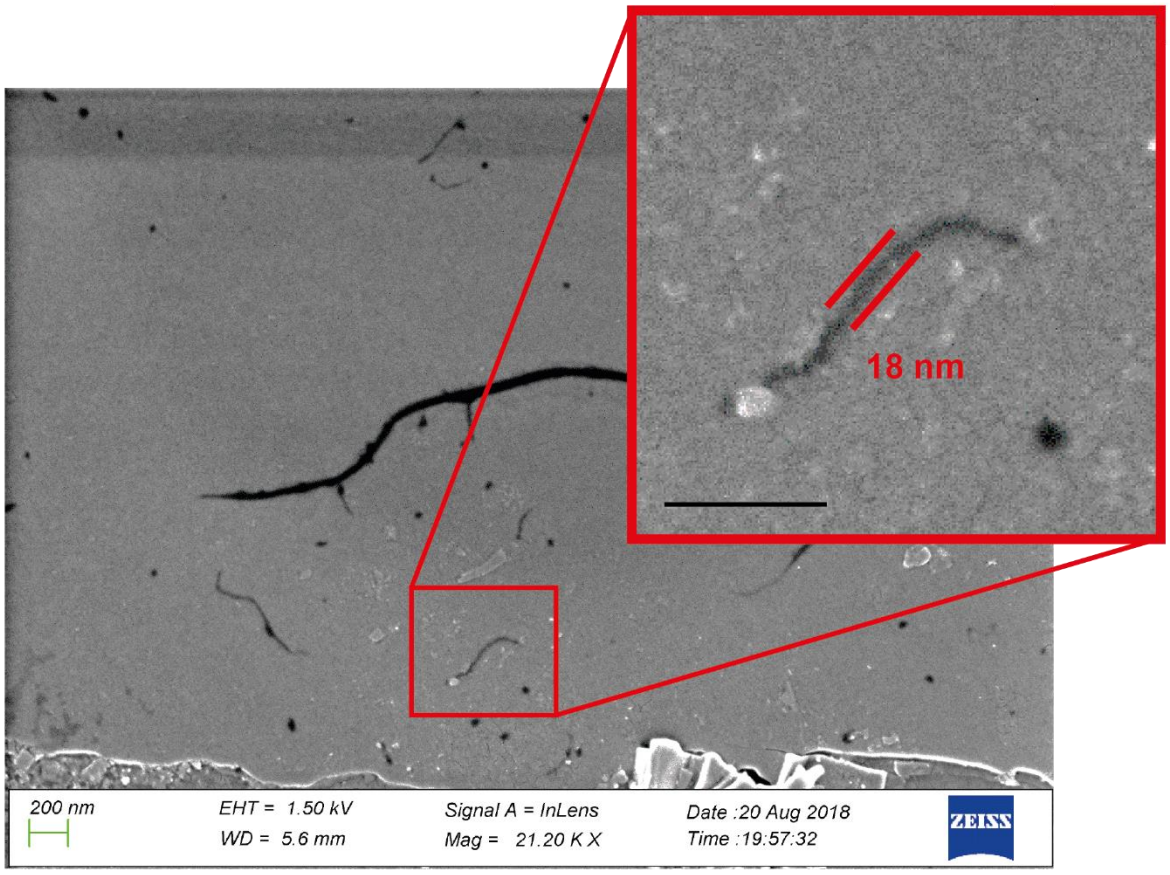

Figure S7. High magnification images of the CNF's width by using negative contrast SEM.

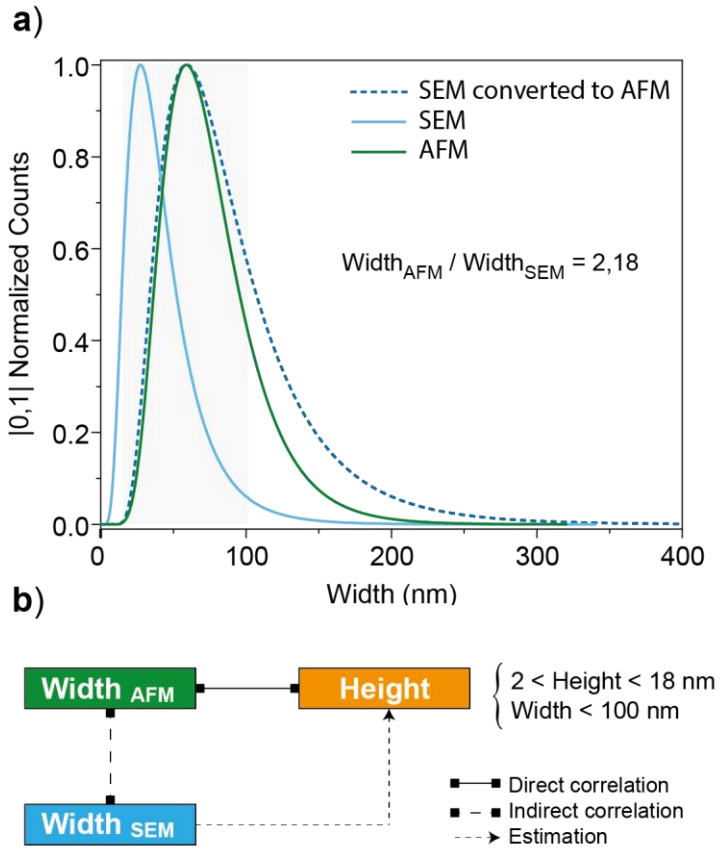

Figure S8. Distribution of widths as obtained from (a) AFM or SEM and corresponding relationship between the two distributions accounting for linear regime, i.e. for widths below 100 nm. (b) Schematic showing the approach to relate AFM and SEM measurements in order to estimate height information from SEM measurement.

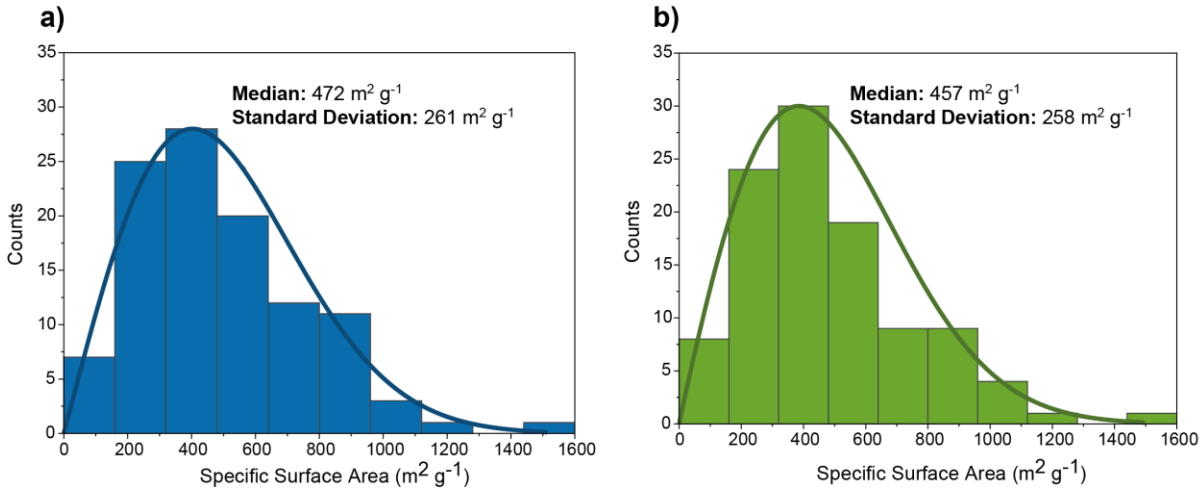

Figure S9. Distribution of the specific surface area calculated using the width, height and length of fibrils. Panel (a) corresponds to SSA values obtained from dimensions based on the SEM (with AFM heights), while (b) stands for SSA values obtained from dimensions acquired in the AFM (with SEM lengths). The relationship between the widths from SEM and AFM, and their corresponding inter-analyzes relations (as described in the main text) were used to obtain all the three dimensions required for the SSA calculations. AFM provided widths that are two-fold bigger than SEM, but this difference did not alter significantly the calculated SSA value, as shown in the panels (a) and (b).

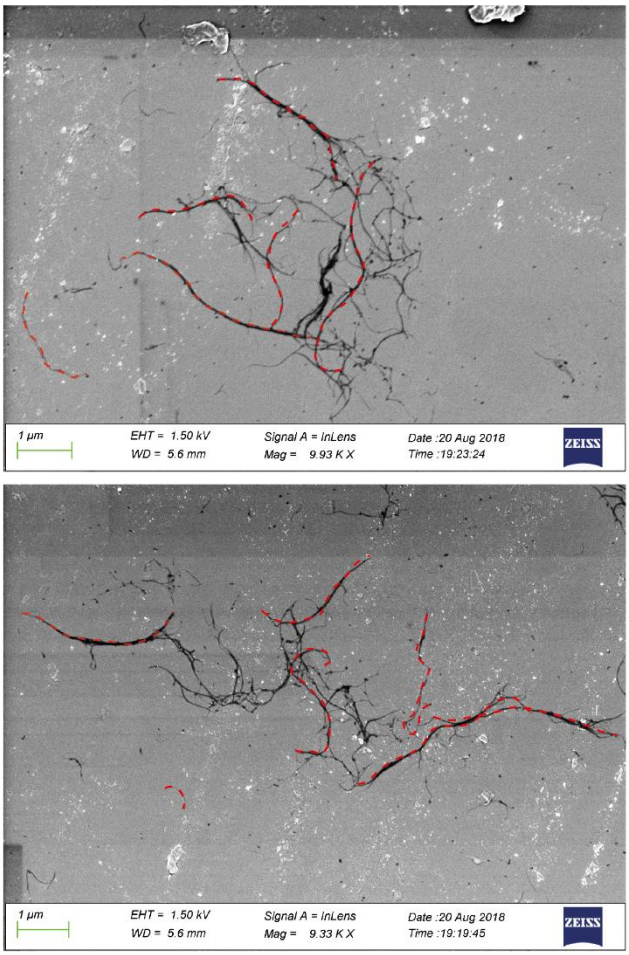

Figure S10. Examples, marked in red dashed line, of the sampling for the measurement of the fibril's length by NegC SEM.